

Molecular modeling and antimycobacterial studies of Mannich bases: 5-hydroxy-2-methyl-4*H*-pyran-4-ones

Barkın BERK¹, Demet US¹, Sinem ÖKTEM², Z. Tanıl KOCAGÖZ²,
Berrak ÇAĞLAYAN³, Işıl AKSAN KURNAZ³, Dilek DEMİR EROL^{1,*}

¹Yeditepe University, Faculty of Pharmacy, Department of Pharmaceutical Chemistry,
34755, Kayışdağı, İstanbul-TURKEY
e-mail: derol@yeditepe.edu.tr.

²Acıbadem University, Faculty of Medicine, Department of Microbiology,
İstanbul-TURKEY

³Yeditepe University, Faculty of Engineering and Architecture, Department of Genetics and Bioengineering,
34755, Kayışdağı, İstanbul-TURKEY

Received 19.06.2010

The World Health Organization lists tuberculosis among the top 3 leading causes of death from a single infectious agent, and reported cases of multidrug-resistant tuberculosis (MDR-TB) are on the rise.

In an attempt to improve MDR-TB drug-directed therapy, we synthesized 11 4-substituted piperazine derivatives of 3-hydroxy-6-methyl-4*H*-pyran-4-one pharmacophore by reacting 5-hydroxy-2-methyl-4*H*-pyran-4-one with suitable piperazine derivatives under Mannich reaction conditions.

Inhibitory effects of the 11 compounds on *Escherichia coli* DNA gyrase were evaluated via DNA gyrase supercoiling assay. The minimum inhibitory concentrations (MIC) of the 11 compounds and 41 compounds from our previous studies against *Mycobacterium tuberculosis* H37RV were assessed, in vitro, by a broth dilution method. To determine the interaction pattern between active site amino acids and all 52 compounds, homology modeling for the construction of *M. tuberculosis* DNA gyrase B subunit was performed, followed by a docking study.

The data presented here could prove useful in future studies on interaction field analysis and high throughput virtual screening of the derivatives of the 3-hydroxy-6-methyl-4*H*-pyran-4-one pharmacophore toward the development of more clinically applicable compounds.

Key Words: Antimycobacterial activity, DNA gyrase activity, hydroxy-4*H*-pyran-4-one, homology modeling

*Corresponding author

Introduction

The World Health Organization estimates that about 8-10 million new tuberculosis (TB) cases occur annually, worldwide. Tuberculosis is listed among the top 3 leading causes of death from a single infectious agent, along with malaria and the human immunodeficiency virus (HIV).¹ In the past decade, it has been reported that the incidence of multidrug-resistant TB (MDR-TB) is on the rise, not only in developing countries but also in industrialized nations.¹ Moreover, enhanced susceptibility to TB in HIV-infected populations and increased cases of the highly contagious and life-threatening pulmonary form of TB pose a serious worldwide health concern. This underscores the importance of the development of new nonresistant anti-TB drugs and new protocols for the efficacious clinical control of TB patients using the antimycobacterial drugs available today.¹

The primary cause of MDR-TB stems from the sophisticated genomic structure of *Mycobacterium tuberculosis*. The *M. tuberculosis* genome comprises 4,411,529 base pairs, contains around 4000 genes, and has a very high guanine and cytosine content that is reflected in the biased amino acid protein content.² *M. tuberculosis* differs radically from other bacteria in that a very large portion of its coding capacity is devoted to the production of enzymes, and it is highly flexible to adaptation and variation.²

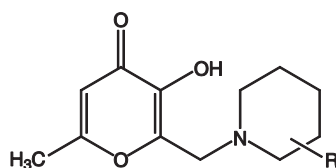
The *M. tuberculosis* genome encodes only 2 topoisomerase-producing genes, one for DNA gyrase, a type II DNA topoisomerase, and the other for topoisomerase I, excluding the topoisomerase IV gene, another type II DNA topoisomerase involved in the DNA replication process. In such cases, DNA gyrase is the only type II enzyme responsible for the negative supercoiling of DNA by relaxing and decatenating positively supercoiled DNA.³

DNA gyrase, which is found in all bacteria, is an adenosine triphosphate (ATP)-dependant hydrolytic enzyme, a proven target for antibacterial chemotherapy.⁴ DNA gyrase comprises two subunits, GyrA and GyrB, forming functional heterodimer A2B2. The GyrA subunit is responsible for DNA breakage and reunion. This catalytic process involves large conformational changes in the enzyme, which are triggered by the binding and hydrolysis of ATP on the GyrB subunit.⁵

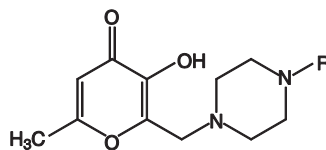
Presently, fluoroquinolones are the only inhibitors of DNA gyrase A commonly used by physicians to treat bacterial infections.⁶⁻⁸ However, reports of fluoroquinolone side effects and toxicity,⁹⁻¹¹ as well as the emergence of bacterial fluoroquinolone resistance,^{7,12} have revived a growing interest in alternative compounds such as inhibitors of the ATPase catalytic domain of DNA gyrase.¹³ The most studied and characterized inhibitors of GyrB are coumarin-like natural antibiotics such as novobiocin, clorobiocin, and cyclothialidines, isolated from *Streptomyces* microorganisms, and synthetic derivatives of triazine and indazole ring structures.⁵ However, all were reported to have either high toxicity or low solubility and permeability during in vivo tests.^{14,15}

X-ray crystallographic studies on DNA gyrase B structural motifs in complex with inhibitors of microorganisms such as *Thermus thermophilus*, *Escherichia coli*, and *Staphylococcus aureus* have been published.¹⁶⁻²⁴ Although these homologs have similar catalytic activities compared to *M. tuberculosis*, the crystallographic structures of *M. tuberculosis* DNA gyrases have not been reported yet.

Compounds derived from 3-hydroxy-4(1H)-pyranone structurally resemble the coumarin ring system^{37,38} and exhibit antimicrobial,²⁵⁻²⁹ antitumor,^{30,31} anticonvulsant,³²⁻³⁴ and tyrosinase inhibitory effects.^{35,36} Previously, various 2-substituted piperazine/piperidine-1-yl-methyl derivatives of 3-hydroxy-6-methyl-4*H*-pyran-4-ones^{37,38} were coupled in compounds **5a-w** and **6a-s**, shown in Tables 1 and 2, respectively,^{33,34,39} and were

Table 1. MIC ($\mu\text{g/mL}$) values determined for the piperidine derivatives against *M. tuberculosis* H37RV.

	R	MIC ($\mu\text{g/mL}$)		R	MIC ($\mu\text{g/mL}$)
6a	hydrogen	16	6j	4-hydroxy	16
6b	2-methyl	64	6k	3-(hydroxymethyl)	32
6c	3-methyl	64	6l	4-(hydroxymethyl)	32
6d	4-methyl	16	6m	4-phenyl	16
6e	2,6-dimethyl	64	6n	4-(4-hydroxyphenyl)	16
6f	3,5-dimethyl	8	6o	4-piperidin-1-yl	16
6g	5-ethyl-2-methyl	64	6p	4-(4-morpholino)	16
6h	4-propyl	16	6r	4-benzyl	16
6i	3-hydroxy	32	6s	4-ethoxycarbonyl	8

Table 2. MIC ($\mu\text{g/mL}$) values determined for the 4-substituted piperazine derivatives against *M. tuberculosis* H37RV.

	R	MIC ($\mu\text{g/mL}$)		R	MIC ($\mu\text{g/mL}$)
4a	2-cyanophenyl	32	5g	4-methylphenyl	16
4b	2-cyanoethyl	32	5h	4-chlorophenyl	8
4c	3,4-dichlorophenyl	32	5i	4-(trifluoromethyl)phenyl	8
4d	4-chlorobenzyl	16	5j	4-cyanophenyl	16
4e	4-hydroxyphenyl	32	5k	4-nitrophenyl	16
4f	2-phenylethyl	64	5l	cyclohexyl	16
4g	2-ethoxyethyl	128	5m	pyridine-2-yl	16
4h	2-methylphenyl	32	5n	pyridine-4-yl	16
4i	prop-2-en-1-yl	64	5o	phenylcarbonyl	16
4j	2-methoxyethyl	128	5p	furan-2-ylcarbonyl	16
4k	propan-2-yl	128	5q	tetrahydrofuran-2-ylmethyl	16
5a	phenyl	8	5r	cyclohexyl methyl	16
5b	2-chlorophenyl	4	5s	N-methylpiperidin-4-yl	8
5c	2-fluorophenyl	16	5t	tert-butoxycarbonyl	8
5d	2-methoxyphenyl	16	5u	ethoxycarbonyl	16
5e	3-chlorophenyl	8	5v	2-hydroxyethyl	16
5f	3-methoxyphenyl	16	5w	2-(dimethylamino)ethyl	16

then screened in vitro for their antimicrobial activities, quantified in MIC ($\mu\text{g/mL}$), against *E. coli*, *S. paratyphi*, *S. flexneri*, *E. gergoviae*, and *Mycobacterium smegmatis* via a broth dilution technique. The MIC results obtained, as low as 4 $\mu\text{g/mL}$ against *M. smegmatis*, were found to be promising, indicating that these structures could potentially have high efficacy in low concentrations against *M. tuberculosis*.^{37,38}

In this study, 11 2-[(4-substitutedpiperazin-1-yl)methyl] derivatives of 3-hydroxy-6-methyl-4*H*-pyran-4-one (compounds **4a-k**, Figure 1 and Table 2) were synthesized and characterized by physicochemical, spectral (IR, ¹H-NMR), and elemental analysis methods. The 11 newly synthesized compounds were screened for supercoiling inhibitory activity by a commercial *E. coli* DNA gyrase supercoiling assay (Figure 2). These compounds were also coupled with 41 previously synthesized 2-substituted piperazine/piperidine-1-yl-methyl derivatives of 3-hydroxy-6-methyl-4*H*-pyran-4-ones.^{33,34,37-39} The desired products were then tested for their antimycobacterial activities against *M. tuberculosis* H37RV via broth dilution to determine their MICs (Tables 1 and 2).

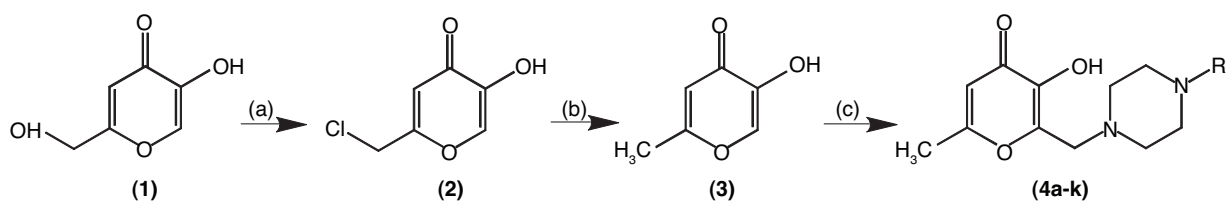


Figure 1. General synthesis of 3-hydroxy-6-methyl-2-[(4-substitutedpiperazin-1-yl)methyl]-4*H*-pyran-4-one derivatives (compounds **4a-k** in Table 2).

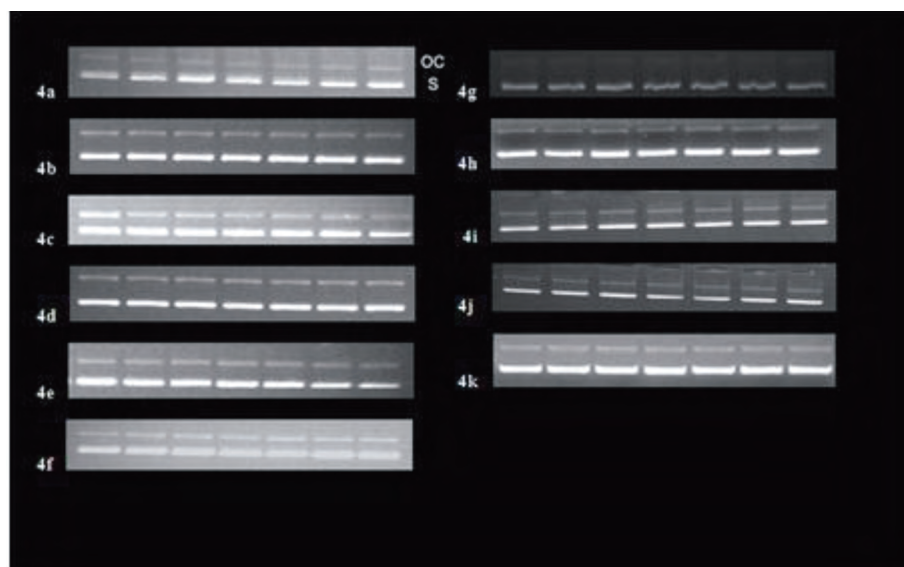


Figure 2. Effects of 11 newly synthesized 3-hydroxy-6-methyl-2-[(4-substitutedpiperazin-1-yl)methyl]-4*H*-pyran-4-one derivatives (compounds **4a-k** in Table 2) on DNA gyrase supercoiling activity. The bands in the agarose gel pictures indicate the topoisomers of the pBR322 plasmid. OC and S indicate the open-circular and supercoiled pBR322 plasmid DNA, respectively.

The structure of the unknown DNA gyrase B chain for *M. tuberculosis* was constructed by the known amino acid sequence of DNA gyrase B for *M. tuberculosis*, available in the UniProtKB database (UniProtKB/Swiss-Prot P0C5C5), and a similar template X-ray crystal structure of the 43 K ATPase domain of *Thermus thermophilus* gyrase B in complex with novobiocin (PDB Code: 1KIJ).⁴⁰ Finally, we performed core-constrained rigid docking experiments using all of the new and previously synthesized compounds to establish structure-activity relations based on activity and modeling data.

Experimental methods

All reagents were obtained from commercial sources. Solvents were dried and purified by known conventional methods. DNA Gyrase Assay Kit 3 (1000U-K0003) and DNA gyrase enzyme (100U-G1001) were purchased from Inspiralis (Norwich, UK). Molecular Operating Environment (MOE 2009.10) (Chemical Computing Group, Montreal, Canada) and Maestro (Schrödinger Corp., Portland, USA) software were used for modeling purposes. Melting points were detected with a Mettler-Toledo FP-62 melting point apparatus (Columbus, USA) and are uncorrected. IR spectra (KBr) were recorded on a Perkin Elmer 1720X FT-IR spectrometer (Beaconsfield, UK). ¹H-NMR spectra were obtained with a Varian Mercury 400, 400 MHz, High Performance Digital FT-NMR using DMSO-d₆, CDCl₃, and CD₃OD as solvents and tetramethylsilane as an internal standard. All chemical shift values (δ) were recorded in ppm. Compound purity was monitored by thin-layer chromatography on silica gel-coated aluminum sheets (Merck, 1.005554, silica gel HF254-361, Type 60, 0.25 mm; Darmstadt, Germany). Elemental analysis of compounds was performed with a LECO CHNS 932 analyzer (LECO Corp., Michigan, USA). Elemental analysis for C, H, and N were within $\pm 0.4\%$ of theoretical values. ¹H-NMR spectra and elemental analysis were performed at the Central Analysis Laboratory of Ankara University, Faculty of Pharmacy, in Ankara, Turkey.

Chemistry

General method for synthesis of 2-(chloromethyl)-5-hydroxy-4*H*-pyran-4-one (compound 2)

Kojic acid (142 g, 2 mol) (compound **1**, Figure 1) was dissolved in thionyl chloride (237 g, 2 mol), followed by stirring for 2 h at room temperature. The resultant yellow solid was filtered and washed with cold petroleum ether. Recrystallization from water gave light yellow crystals (115 g, 72%), mp 146-147 °C (lit. value⁴¹ 146-147 °C). ¹H-NMR δ (ppm, DMSO-d₆), 9.32 (s, 1H), 8.13 (s, 1H), 6.57 (s, 1H), 4.66 (s, 2H). Anal. Cal. For. C₆H₅ClO₃: C 44.88, H 3.14. Found: C 44.62, H 3.03.

General method for synthesis of 5-hydroxy-2-methyl-4*H*-pyran-4-one (compound 3)

Compound **2** (20 g, 0.12 mol) was suspended in water (500 mL). The temperature of the reaction mixture was raised to 50 °C. Zinc dust (16 g, 0.24 mol) was added and stirred at 70 °C for 30 min. Concentrated hydrochloric acid (13.6 g, 3 mol) was added dropwise, followed by stirring for 3 h at 70 °C. The solution was filtered, poured into ice water, extracted with dichloromethane, dried with anhydrous sodium sulfate, and evaporated to dryness. Recrystallization of the resulting yellow solid from isopropanol yielded compound **3** as light yellow needles (10.2 g, 64%), mp 125-127 °C (lit. value⁴¹ 125-127 °C). ¹H-NMR δ (ppm, DMSO-d₆),

8.96 (s, 1H), 7.97 (s, 1H), 6.24 (s, 1H), 2.24 (s, 3H). Anal. Cal. For. $C_6H_6O_3$: C 57.14, H 4.80. Found: C 57.35, H 4.67.

General method for synthesis of 3-hydroxy-6-methyl-2-[(4-substitutedpiperazin-1-yl)methyl]-4H-pyran-4-one derivatives (compounds 4a-k, Figure 1, Table 2)

A mixture of 0.01 mol of 4-substituted piperazine and 0.01 mol of compound **3** (Figure 1) in 20 mL of methanol with 0.012 mol of 37% formalin was stirred at room temperature until a solid mass precipitated. The compound was filtered and washed with cold water, dried under a vacuum, and recrystallized from suitable solvents.

2-{4-[(3-Hydroxy-6-methyl-4-oxo-4H-pyran-2-yl)methyl]piperazin-1-yl}benzotrile (compound 4a)

Recrystallized from methanol. Mp 158.0 °C. IR (KBr) (ν , cm^{-1} , stretching), 2218 ($C\equiv N$), 1614 ($C=O$), 1452 ($C=C$), 1218 ($C-O$); 1H -NMR δ (ppm, $CDCl_3$), 7.55-7.49 (m, 4H), 6.23 (s, 1H), 3.72 (s, 2H), 3.26 (t, $J = 4.4$ Hz, 4H), 2.83 (t, $J = 4.8$ Hz, 4H), 2.32 (s, 3H). Anal. Cal. For. $C_{18}H_{19}N_3O_3$: C 66.45, H 5.89, N 12.91. Found: C 66.34, H 5.85, N 12.65.

3-{4-[(3-Hydroxy-6-methyl-4-oxo-4H-pyran-2-yl)methyl]piperazin-1-yl}propanenitrile (compound 4b)

Recrystallized from methanol. Mp 120.4 °C. IR (KBr) (ν , cm^{-1} , stretching), 2244 ($C\equiv N$), 1620 ($C=O$), 1454 ($C=C$), 1197 ($C-O$); 1H -NMR δ (ppm, $CDCl_3$), 6.21 (s, 1H), 3.65 (s, 2H), 2.72-2.49 (m, 12H), 2.30 (s, 3H). Anal. Cal. For. $C_{14}H_{19}N_3O_3$: C 60.63, H 6.91, N 15.15. Found: C 60.73, H 6.80, N 14.96.

2-{[4-(3,4-Dichlorophenyl)piperazin-1-yl]methyl}-3-hydroxy-6-methyl-4H-pyran-4-one (compound 4c)

Recrystallized from methanol. Mp 178.5 °C. IR (KBr) (ν , cm^{-1} , stretching), 1626 ($C=O$), 1455 ($C=C$), 1222 ($C-O$); 1H -NMR δ (ppm, $CDCl_3$), 7.27 (m, 1H), 6.94 (d, $J = 2.8$ Hz, 1H), 6.72 (m, 1H), 6.24 (s, 1H), 3.69 (s, 2H), 3.19 (t, $J = 4.8$ Hz, 4H), 2.73 (t, $J = 4.8$ Hz, 4H), 2.32 (s, 3H). Anal. Cal. For. $C_{17}H_{18}Cl_2N_2O_3 \cdot 0.25HOH$: C 54.63, H 4.99, N 7.50. Found: C 54.64, H 5.20, N 7.69.

2-{[4-(4-Chlorobenzyl)piperazin-1-yl]methyl}-3-hydroxy-6-methyl-4H-pyran-4-one (compound 4d)

Recrystallized from methanol/diethyl ether. Mp 159.9 °C. IR (KBr) (ν , cm^{-1} , stretching), 1619 ($C=O$), 1456 ($C=C$), 1199 ($C-O$); 1H -NMR δ (ppm, $CDCl_3$), 7.26 (dd, $J = 8.2$ Hz, 4H), 6.20 (s, 1H), 3.64 (s, 2H), 3.47 (s, 2H), 2.63 (s, 4H), 2.49 (s, 4H), 2.84 (s, 3H). Anal. Cal. For. $C_{18}H_{21}ClN_2O_3 \cdot 0.2HOH$: C 61.34, H 6.12, N 7.95. Found: C 61.38, H 6.24, N 8.00.

3-Hydroxy-2-{[4-(4-hydroxyphenyl)piperazin-1-yl]methyl}-6-methyl-4*H*-pyran-4-one (compound 4e)

Recrystallized from methanol. Mp 178.9 °C. IR (KBr) (ν , cm^{-1} , stretching), 1624 (C=O), 1510 (C=C), 1220 (C-O); $^1\text{H-NMR}$ δ (ppm, CD_3OD), 6.78 (dd, $J = 9.2$ Hz, 4H), 6.26 (s, 1H), 3.73 (s, 2H), 3.06 (t, $J = 4.8$ Hz, 4H), 2.76 (t, $J = 4.8$ Hz, 4H), 2.34 (s, 3H). Anal. Cal. For. $\text{C}_{17}\text{H}_{20}\text{N}_2\text{O}_4$: C 64.54, H 6.37, N 8.86. Found: C 64.19, H 6.34, N 8.82.

3-Hydroxy-6-methyl-2-{[4-(2-phenylethyl)piperazin-1-yl]methyl}-4*H*-pyran-4-one (compound 4f)

Recrystallized from chloroform/*n*-hexane. Mp 182.9 °C. IR (KBr) (ν , cm^{-1} , stretching), 1626 (C=O), 1432 (C=C), 1223 (C-O); $^1\text{H-NMR}$ δ (ppm, CDCl_3), 7.24 (m, 5H), 6.20 (s, 1H), 3.67 (s, 2H), 2.80-2.60 (m, 12H), 2.29 (s, 3H). Anal. Cal. For. $\text{C}_{19}\text{H}_{24}\text{N}_2\text{O}_3$: C 69.49, H 7.37, N 8.53. Found: C 69.13, H 7.35, N 8.33.

2-{[4-(2-Ethoxyethyl)piperazin-1-yl]methyl}-3-hydroxy-6-methyl-4*H*-pyran-4-one (compound 4g)

Recrystallized from methanol/diethyl ether. Mp 133.0 °C. IR (KBr) (ν , cm^{-1} , stretching), 1626 (C=O), 1450 (C=C), 1108 (C-O); $^1\text{H-NMR}$ δ (ppm, CDCl_3), 6.20 (s, 1H), 3.66 (s, 2H), 3.56-3.46 (m, 4H), 2.66-2.58 (m, 10H), 2.29 (s, 3H), 1.19 (t, $J = 7.2$ Hz, 3H). Anal. Cal. For. $\text{C}_{15}\text{H}_{24}\text{N}_2\text{O}_4$: C 60.79, H 8.16, N 9.45. Found: C 60.58, H 8.34, N 9.16.

3-Hydroxy-6-methyl-2-{[4-(2-methylphenyl)piperazin-1-yl]methyl}-4*H*-pyran-4-one (compound 4h)

Recrystallized from ethyl acetate/diethyl ether. Mp 220.7 °C. IR (KBr) (ν , cm^{-1} , stretching), 1617 (C=O), 1437 (C=C), 1224 (C-O); $^1\text{H-NMR}$ δ (ppm, CDCl_3), 7.15 (m, 4H), 6.33 (s, 1H), 4.36 (s, 2H), 3.65 (s, 4H), 3.17 (s, 4H), 2.44 (s, 3H), 2.27 (s, 3H). Anal. Cal. For. $\text{C}_{18}\text{H}_{22}\text{N}_2\text{O}_3 \cdot 2.5\text{HOH}$: C 60.15, H 7.57, N 7.79. Found: C 60.27, H 7.05, N 7.63.

3-Hydroxy-6-methyl-2-{[4-(prop-2-en-1-yl)piperazin-1-yl]methyl}-4*H*-pyran-4-one (compound 4i)

Recrystallized from methanol/diethyl ether. Mp 152.2 °C. IR (KBr) (ν , cm^{-1} , stretching), 1616 (C=O), 1456 (C=C), 1201 (C-O); $^1\text{H-NMR}$ δ (ppm, CDCl_3), 6.20 (s, 1H), 5.87-5.80 (m, 1H), 5.21-5.14 (m, 2H), 3.66 (s, 2H), 3.01 (d, $J = 6.4$ Hz, 2H), 2.70-2.50 (m, 8H), 2.29 (s, 3H). Anal. Cal. For. $\text{C}_{14}\text{H}_{20}\text{N}_2\text{O}_3$: C 63.62, H 7.63, N 10.60. Found: C 63.38, H 7.89, N 10.37.

3-Hydroxy-2-{[4-(2-methoxyethyl)piperazin-1-yl]methyl}-6-methyl-4*H*-pyran-4-one (compound 4j)

Recrystallized from methanol/diethyl ether. Mp 135.0 °C. IR (KBr) (ν , cm^{-1} , stretching), 1660 (C=O), 1458 (C=C), 1111 (C-O); $^1\text{H-NMR}$ δ (ppm, CDCl_3), 6.20 (s, 1H), 3.66 (s, 2H), 3.50 (t, $J = 5.6$ Hz, 2H), 3.45 (s, 3H), 2.59 (t, $J = 5.6$ Hz, 2H), 2.70-2.60 (m, 8H), 2.29 (s, 3H). Anal. Cal. For. $\text{C}_{14}\text{H}_{22}\text{N}_2\text{O}_4 \cdot 0.17\text{HOH}$: C 58.93, H 7.89, N 9.82. Found: C 58.97, H 7.74, N 9.75.

3-Hydroxy-6-methyl-2-{[4-(propan-2-yl)piperazin-1-yl]methyl}-4*H*-pyran-4-one (compound 4k)

Recrystallized from ethyl acetate/diethyl ether. Mp 153.2 °C. IR (KBr) (ν , cm^{-1} , stretching), 1626 (C=O), 1453 (C=C), 1199 (C-O); $^1\text{H-NMR}$ δ (ppm, CDCl_3), 6.19 (s, 1H), 3.66 (s, 2H), 2.67 (m, 1H), 2.65-2.55 (m, 8H), 2.28 (s, 3H), 1.04 (d, $J = 6.8$ Hz, 6H). Anal. Cal. For. $\text{C}_{14}\text{H}_{22}\text{N}_2\text{O}_3$: C 63.13, H 8.33, N 10.52. Found: C 63.26, H 7.91, N 10.46.

Molecular modeling

Homology modeling of *M. tuberculosis* DNA gyrase subunit B was carried out by Chemical Computing Group MOE software, version 2009.10, based on the crystal structure of the 43 K ATPase domain of *Thermus thermophilus* gyrase B in complex with novobiocin (PDB code 1KIJ, 2.30 Å resolution, 43% identity among 420 aligned residues).⁴⁰

The target sequence was located in the UniProtKB/Swiss-Prot database (access number P0C5C5). The sequence alignment and homology modeling were performed using MOE-align and MOE-homology model modules. During the modeling process, the position of crystallized novobiocin and a water molecule, which was believed to be responsible for key interactions, were kept in their original positions for rebuilding the binding cavity in the specific and original size. Subsequently, hydrogen ligands were removed from this model file and subjected to a protein preparation wizard: Maestro for hydrogen adjustment and rotamers, and H-bond optimization using OPLS 2005 as the energy parameters. Grid files were prepared without restrictions in the Glide-Grid application of Maestro. Ligand structures enriched with novobiocin were prepared for their tautomeric and ionized forms at various pH levels using the Lig Prep function of Maestro, followed by Glide docking using XP mode with the restricted coumarin core of novobiocin. Compound poses with the most negative e-model scores, which consider hydrophobic parameters extensively, were selected and analyzed visually.

Microbiology

Broth dilution method for Minimum Inhibitory Concentration (MIC)

MICs of compound preparations were determined by broth dilution using Middlebrook 7H10 agar supplemented with 10% oleic acid–albumin–dextrose–catalase for mycobacteria and tryptic soy broth for other species. The tested dilutions ranged from 128 to 0.5 $\mu\text{g}/\text{mL}$ using dimethyl sulfoxide (DMSO) as the solvent for all compounds. *Mycobacteria* were suspended in Middlebrook 7H10 broth and the others in tryptic soy broth to match the turbidity of 1 McFarland standard (2×10^8 cfu/mL). Tube slants were inoculated with undiluted or 1/100 diluted bacterial suspensions and incubated at 37 °C. The slants were examined until visible colonies were observed in the control tube. Controls prepared with concentrations of DMSO used in the dilutions did not show any inhibitory activity under these circumstances. The MIC value of each isolate was the lowest concentration of the compound that inhibited visible bacterial growth.

DNA gyrase supercoiling assay

DNA gyrase supercoiling assays were performed with a Gyrase Supercoiling Assay Kit (Inspiralis) according to the manufacturer's instructions and analyzed by monitoring the conversion of relaxed pBR322 plasmid to its supercoiled form using DNA gel electrophoresis. Essentially, 1 U of *E. coli* DNA gyrase was first diluted in 5 × gyrase buffer and incubated in an assay buffer (35 mM Tris HCl (pH 7.5), 24 mM KCl, 4 mM MgCl₂, 2 mM DTT, 1.8 mM spermidine, 1 mM ATP, 6.5% (w/v) glycerol, and 0.1 mg/mL BSA), with 0.5 μg of pBR322 plasmid and a series of synthesized compound dilutions at 37 °C for 30 min. Reactions were stopped with the addition of stop dye (40% sucrose, 100 mM Tris HCl (pH 7.5), 1 mM EDTA, and 0.5 mg/mL bromophenol blue) and loaded onto TAE agarose gel (1%). Gels were visualized using a gel documentation system (Bio-Rad ChemiDoc). Since high levels of DMSO are known to affect DNA gyrase activity, titration was used to determine the minimum amount of DMSO to be used in the assays, and 5% DMSO (with negligible or no effect on the gyrase) was chosen to dilute the compounds (data not shown); see Tables 1 and 2.

Results and discussion

The synthesis of key intermediate 5-hydroxy-2-methyl-4*H*-pyran-4-one (compound **3**), available from the extensively studied methyl side chain chlorination of kojic acid with thionyl chloride followed by selective reduction of the chloro atom in the presence of zinc dust, was undertaken.^{32–34,41,42}

With the process outlined above, compound **3** (allomaltol, in nonsystematic nomenclature) was produced, without affecting the hydroxyl group at the fifth position of 2-(chloromethyl)-5-hydroxy-4*H*-pyran-4-one (compound **2**), in moderate yields. Finally, the targeted 3-hydroxy-6-methyl-2-((4-substitutedpiperazin-1-yl)methyl)-4*H*-pyran-4-one derivatives (compounds **4a-k**) shaped the reacting allomaltol with suitable piperazine derivatives in a methanol/formalin medium until formation of the desired precipitates at room temperature was achieved. In the Mannich reaction, substitution for the second position of the ring system is preferred due to the presence of a free enolic hydroxyl group in the third position.⁴³ Compounds were crystallized from appropriate solvents in moderate yields.

By IR, ¹H-NMR, and elemental analysis, 11 compounds were characterized. In the IR spectra, the C=O stretch band belonging to the fourth position of the pyran ring was generally seen between 1614 and 1660 cm⁻¹. C-H stretching belonging to the methyl group at the sixth position of the pyran and piperazine ring system was observed between 2800 and 2900 cm⁻¹. In combination with the side chains, the pyran ring's C=C stretching bands were observed at 1432-1510 cm⁻¹ and the C-O-C stretching of the pyran system was noticeable between 1108 and 1224 cm⁻¹. The C≡N stretching in the functional side of compounds **6a** and **6b** was observed at 2214-2244 cm⁻¹.

In the ¹H-NMR spectra of the compounds, piperazine ring protons were seen at δ 2.49-3.65 ppm. Side chain hydrogens and sixth-position methyl protons were seen at δ 1.04-2.84 ppm in consensus with the total number of hydrogens. Vinylic protons of the pyran ring system were observed as singlets at δ 6.20-6.33 ppm. Hydroxyl protons of the ring system changed with deuterated solvents and were not observed. The methylene linkage protons between the pyran and piperazine rings were between δ 3.64 and 4.36 ppm as singlets. The removal of the singlet around 9-9.5 ppm belonging to the proton at the sixth position of the allomaltol structure and the formation of these new singlets confirmed the desired 3-hydroxy-6-methyl-2-[(4-substitutedpiperazin-

1-yl)methyl]-4*H*-pyran-4-one structures. All other protons were observed according to the expected chemical shift and integral values.^{32,33,44}

Based on previously published procedures, we screened the synthesized compounds' inhibitory effects on supercoiling by performing DNA gyrase supercoiling assays, using gel electrophoresis and *E. coli* gyrase, which can convert relaxed pBR322 plasmids to their supercoiled topoisomer.^{45,46} In these procedures, DNA gyrase activity can be monitored as 2 or more bands on an agarose gel where the upper band is an open-circular (nicked) plasmid and the faster running band is a negatively supercoiled (closed-circular) plasmid. The inhibition of gyrase supercoiling was visually assessed by a 50% reduction of the supercoiled band and the appearance of a spread of slower migrating plasmids. In our previous studies, we reported the inhibitory effects of compounds **5a-6s**.^{37,38} Here we report the results for the inhibition of gyrase supercoiling assay of newly synthesized compounds **4a-k** (Figure 2). All screened piperidine and piperazine derivatives of 3-hydroxy-6-methyl-4*H*-pyran-4-one derivatives, including those newly synthesized, revealed mild to moderate inhibitor activity on *E. coli* DNA gyrase supercoiling.

Sequence similarities between DNA gyrase B subunits of *E. coli* and *M. tuberculosis* (UniProtKB/Swiss-Prot database accession numbers P0AES7 and P0C5C5, respectively) suggested a 48% overall score after alignment with ClustalW2.⁴⁷ The combination of DNA gyrase supercoiling assay results and this finding provoked us to investigate the inhibition potencies of these compounds in vitro.

Minimum inhibitory concentrations values for the 52 compounds were assessed with *M. tuberculosis* H37RV, using a gradient-based decreasing concentration technique by the broth dilution method. The lowest MIC (4 µg/mL) was attributed to compound **5b**, structured as 2-((4-(2-chlorophenyl)piperazin-1-yl)methyl)-3-hydroxy-6-methyl-4*H*-pyran-4-one. For other compounds, the MIC results were also promising: between 8 and 128 µg/mL weighted at a 16 µg/mL concentration.

4-Substituted-piperazinyl derivatives (**5a-v** and **4a-k**) varied in their antimycobacterial effects with diverse substitutions. 4-Phenyl (**5a**), 4-(*N*-methylpiperidin-4-yl) (**5s**), and 4-*tert*-butoxycarbonyl (**5t**) substitutions of the piperazine core resulted in MIC values of 8 µg/mL. Various 2-, 3-, 4-, and 5-phenyl side chain substitutions revealed decreasing potency, whereas, on the contrary, the 4-(2-chlorophenyl) derivative **5b** acted as an inhibitor. Placing a linker of 2 or 3 carbons between the piperazine core and the phenyl group (**4d-f**) led to a decline in inhibitor activity. Interestingly, the largest decrease in potency was observed with 4-(2-ethoxyethyl) (**4g**) and 4-(2-methoxymethyl) (**4j**) substituted piperazine derivatives.

For substituted piperidine derivatives **6a-s**, 2- or 6-positioned side chain substitutions mainly reduced the inhibitory activity against *M. tuberculosis*, while 3- and 5-positioned side chain substitutions revealed higher activity than a nonsubstituted piperidine ring. When compared to 3- and 5-substituted piperidines, substitution from the fourth position of the piperidine ring revealed a potency of 8 µg/mL, similar to 4-ethoxycarbonylpiperidine derivative **6s**.

To examine the possible interactions between ligands and the active site of the *Mycobacterium* DNA gyrase B subunit, homology modeling and a docking process were undertaken.

For homology modeling of the DNA gyrase subunit B of *M. tuberculosis*, the crystal structure of the gyrase B 43 K ATPase domain complex with the potent inhibitor novobiocin (PDB code 1KIJ)²³ was selected as the template. This "open" conformation of the active site in the absence of ATP is unique, as it clearly demonstrates large conformational changes during inhibition processes.

This crystal structure has a special water molecule (HOH 539) trapped in the hydrophobic cavity that shows a clear H-bonding network with Asp 72 (a key amino acid responsible for the activity), Gly 76, Thr 166, and the ligand itself. We selected this template to preserve this particular H-bonding network of amino acid-water molecule-ligand within the modeling process.¹⁷ Even if there were other better E-valued crystal structures according to the compositional matrix adjusted alignment of BLAST-p, we would still have selected this particular template.

During homology modeling, after the heavy atoms were modeled and all hydrogen atoms were added, the protein coordinates were minimized with MOE using the AMBER94 force field.⁴⁸ Protein stereochemistry evaluation was performed using several tools (Ramachandran and Chi plots to measure phi/psi and chi1/chi2 angles and clash contact reports) implemented in the MOE suite.⁴⁹ The pair-wise percentage residue identity was determined as 46.4 between 2 chains, where the pair-wise RMSD values for C α and the main chain backbone atoms of the superimposed model and template were 0.64 and 0.70 Å, respectively.

Briefly, the structure comprised a compact single domain with an 8-stranded beta sheet, which was flanked on 1 side by 3 alpha-helices and random coils. By keeping the conserved water molecule and novobiocin during the modeling process, we not only preserved the appropriate distances and hydrogen networking between the key amino acids of the active site, but also tried to steadily preserve the binding mode of novobiocin. The RMSD value difference of 0.84 Å of the pose from the nonrestricted redocking of the novobiocin structure itself also confirmed the approach.

The coiled “open” protein structure gave the active site a considerable amount of flexibility, which could also affect the binding mode of the ligands. Considering the structural resemblance between 3-hydroxy-4(1H)-pyranone and the coumarin ring system, we performed the docking core under restriction. The docking poses belonging to ligands suggested that Arg 82 stabilized the sixth-position methyl group over the pyranone ring system with hydrophobic interactions, whereas bridge methyl, piperidine, and piperazine carbons were stabilized between Phe 109 and Ile 84 with the same kind of interactions. The substituted phenyl structures were generally positioned in the hydrophobic space surrounded by Val 99, Val 125, Val 123, Ile 84, and Asn 52. If there is a hydrogen donating group in the para position of phenyl, then there is a chance of a hydrogen bond existing with that group and the Val 123 carbonyl. The small groups, such as hydroxymethyl, in the third position of the piperidine ring have a tendency to form a hydrogen bond with the carbon Asp 52 backbone carbonyl and the conserved water molecule (Figure 3).

Although the generated docking poses illustrated a parallelism between MIC values against *M. tuberculosis* and compound interactions with the surrounding environment regarding side chain changes in general, further molecular dynamics simulations for this computationally estimated crystal structure of the complex, under physiological conditions, would be the best option for verification.

Both piperidine and piperazine derivatives of 3-hydroxy-6-methyl-4*H*-pyran-4-one pharmacophore are promising compounds for MDR-TB; their high efficiency toward particular *M. tuberculosis* strains is comparable to standard novobiocin.⁵⁰ An alternative to finding a core other than 5-hydroxy-2-methyl-4*H*-pyran-4-one would be to perform high throughput virtual screening methods using a homology model of *M. tuberculosis* DNA gyrase B together with side-chain interaction field analysis over existing piperidine and piperazine side chains to evaluate more clinically applicable compounds.

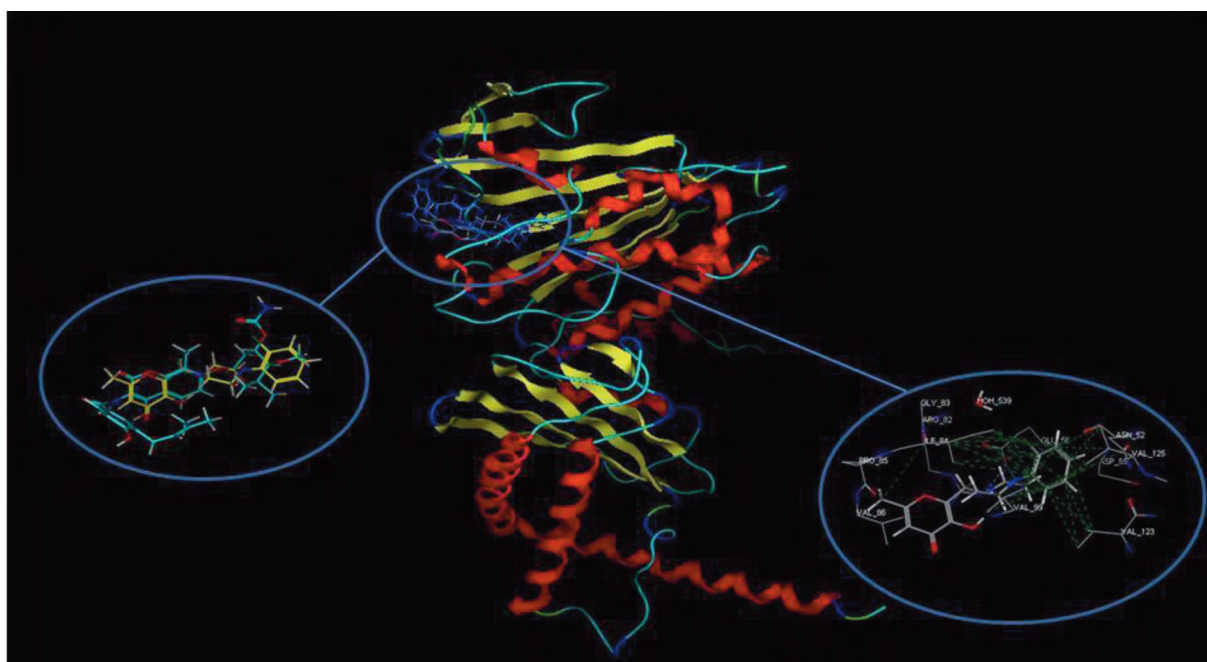


Figure 3. Docked coordinates of compound **5b** and novobiocin in the active site (circled in the upper middle) of the homology model of *M. tuberculosis* DNA gyrase B. The circle on the left shows compound **5** (yellow) superposed with novobiocin (green). The circle on the right shows hydrophobic (green dotted lines) and electrostatic (blue dotted lines) interactions between compound **5** and the amino acid residues of the binding site.

Acknowledgement

We thank Shirley McCartney, Ph.D., for proofreading and discussion.

References

1. Tomioka, H.; Namba, K. *Kekkaku* **2006**, *81*, 753-774.
2. Cole, S.; Brosch, R.; Parkhill, J.; Garnier, T.; Churcher, C.; Harris, D.; et al. *Nature* **1998**, *393*, 537-544.
3. Champoux, J. J. *Annu. Rev. Biochem.* **2001**, *70*, 369-413.
4. Ferrero, L.; Cameron, B.; Manse, B.; Lagneaux, D.; Crouzet, J.; Famechon, A.; Blanche, F. *Mol. Microbiol.* **1994**, *13*, 641-653.
5. Maxwell, A. *Trends Microbiol.* **1997**, *5*, 102-109.
6. Drlica, K.; Malik, M. *Curr. Top. Med. Chem.* **2003**, *3*, 249-282.
7. Mitscher, L. A. *Chem. Rev.* **2005**, *105*, 559-592.
8. Sifaoui, F.; Lamour, V.; Varon, E.; Moras, D.; Gutmann, L. *J. Bacteriol.* **2003**, *185*, 6137-6146.
9. Stahlmann, R. *Toxicol. Lett.* **2002**, *127*, 269-277.

10. Leone, R.; Venegoni, M.; Motola, D.; Moretti, U.; Piazzetta, V.; Cocci, A.; Resi, D.; Mozzo, F.; Velo, G.; Burzillieri, L.; Montanaro, N.; Conforti, A. *Drug Saf.* **2003**, *26*, 109-120.
11. Oh, Y. R.; Carr-Lopez, S. M.; Probasco, J. M.; Crawley, P. G. *Ann. Pharmacother.* **2003**, *37*, 1010-1013.
12. Piddock, L. J. V. *Drugs* **1999**, *58*, 11-18.
13. Maxwell, A.; Lawson, D. M. *Curr. Top. Med. Chem.* **2003**, *3*, 283-303.
14. Boehm, H.; Boehringer, M.; Bur, D.; Gmuender, H.; Huber, W.; Klaus, W.; Kostrewa, D.; Kuehne, H.; Luebbers, T.; Meunier-Keller, N.; Mueller, F. *J. Med. Chem.* **2000**, *43*, 2664-2674.
15. Poyser, J. P.; Telford, B.; Timms, D.; Block, M. H.; Hales, N. J. WO Patent 99/01442, 1999.
16. Wigley, D.; Davies, G.; Dodson, E.; Maxwell, A.; Dodson, G. *Nature* **1991**, *351*, 624-629.
17. Lewis, R.; Singh, O.; Smith, C.; Skarzynski, T.; Maxwell, A.; Wonacott, A.; Wigley, D. *EMBO J.* **1996**, *15*, 1412-1420.
18. Holdgate, G.; Tunnicliffe, A.; Ward, W.; Weston, S.; Rosenbrock, G.; Barth, P.; Taylor, I.; Pauptit, R.; Timms, D. *Biochemistry* **1997**, *36*, 9663-9673.
19. Tsai, F.; Singh, O.; Skarzynski, T.; Wonacott, A.; Weston, S.; Tucker, A.; Pauptit, R.; Breeze, A.; Poyser, J.; O'Brien, R.; Ladbury, J.; Wigley, D. *Proteins* **1997**, *28*, 41-52.
20. Brino, L.; Urzhumtsev, A.; Mousli, M.; Bronner, C.; Mitschler, A.; Oudet, P.; Moras, D. *J. Biol. Chem.* **2000**, *275*, 9468-9475.
21. Ward, W.; Holdgate, G. *Prog. Med. Chem.* **2001**, *38*, 309-376.
22. Lafitte, D.; Lamour, V.; Tsvetkov, P. O.; Makarov, A. A.; Klich, M.; Deprez, P.; Moras, D.; Briand, C.; Gilli, R. *Biochemistry* **2002**, *41*, 7217-7223.
23. Lamour, V.; Hoermann, L.; Jeltsch, J.; Oudet, P.; Moras, D. *J. Biol. Chem.* **2002**, *277*, 18947-18953.
24. Bellon, S.; Parsons, J.; Wei, Y.; Hayakawa, K.; Swenson, L.; Charifson, P.; Lippke, J.; Aldape, R.; Gross, C. *Antimicrob. Agents Chemother.* **2004**, *48*, 1856-1864.
25. Kayahara, H.; Shibata, N.; Tadasa, K.; Maeda, H.; Kotani, T.; Ichimoto, I. *Agric. Biol. Chem.* **1990**, *54*, 2441-2442.
26. Kotani, T.; Ichimoto, I.; Tatsumi, C.; Fujita, T. *Agric. Biol. Chem.* **1975**, *39*, 1311-1317.
27. Aytemir, M. D.; Hider, R. C.; Erol, D. D.; Özalp, M.; Ekizoğlu, M. *Turk. J. Chem.* **2003**, *27*, 445-452.
28. Aytemir, M. D.; Erol, D. D.; Hider, R. C.; Özalp, M. *Turk. J. Chem.* **2003**, *27*, 757-764.
29. Wan, H. M.; Chen, C. C.; Giridhar, R.; Chang, T. S.; Wu, W. T. *J. Ind. Microbiol. Biotechnol.* **2005**, *32*, 227-233.
30. Yamato, M.; Yasumoto, Y.; Sakai, J.; Luduena, R. F.; Baneerjee, A.; Tashiro, T. *J. Med. Chem.* **1987**, *30*, 1897-1900.
31. Tamura, T.; Mitsumori, K.; Totsuka, Y.; Wakabayashi, K.; Kido, R.; Kasai, H.; Nasu, M.; Hirose, M. *Toxicology* **2006**, *222*, 213-224.
32. Aytemir, M. D.; Çalıř, Ü.; Özalp, M. *Arch. Pharm. Pharm. Med. Chem.* **2004**, *337*, 281-288.
33. Aytemir, M. D.; Çalıř, Ü. *Hacettepe University Journal of the Faculty of Pharmacy* **2007**, *27*, 1-10.
34. Aytemir, M. D.; Çalıř, Ü. *FABAD J. Pharm. Sci.* **2006**, *31*, 23-29.
35. Cabanes, J.; Chazarra, S.; Garcia-Carmona, F. *J. Pharm. Pharmacol.* **1994**, *46*, 982-985.
36. Kim, H.; Choi, J.; Cho, J. K.; Kim, S. Y.; Lee, Y. S. *Bioorg. Med. Chem. Lett.* **2004**, *14*, 2843-2846.

37. Us, D.; Gürdal, E.; Berk, B.; Öktem, S.; Kocagöz, T.; Çağlayan, B.; Kurnaz, I. A.; Erol, D. D. *Turk. J. Chem.* **2009**, *33*, 803812.
38. Us, D.; Berk, B.; Gürdal, E.; Aytakin, N.; Kocagöz, T.; Çağlayan, B.; Kurnaz, I. A.; Erol, D. D. *Turk. J. Chem.* **2010**, *34*, 447-456.
39. İskeleli, N. O.; Isıka, S.; Aytemir, M. D. *Acta Crystallogr. Sect. E* **2005**, *61*, o1947o1949.
40. Lamour, V.; Hoermann, L.; Jeltsch, J.; Oudet, P.; Moras, D. *J. Biol. Chem.* **2002**, *277*, 18947-18953.
41. Erol, D. D.; Yuluğ, N. *Eur. J. Med. Chem.* **1994** *29* 893-897.
42. Yabuta, T. *J. Chem. Soc.* **1924**, *125*, 575-587.
43. O'Brien, G.; Patterson, J. M.; Meadow, J. R. *J. Org. Chem.* **1960**, *25*, 86-89.
44. Liu, Z. D.; Piyamongkol, S.; Liu, D. Y.; Khodr, H. H.; Lu, S. H.; Hider, R. C. *Bioorg. Med. Chem.* **2001**, *9*, 563-573.
45. Maxwell, A.; Burton, N. P.; O'Hagan, N. *Nucleic Acids Res.* **2006**, *34*, e104.
46. Reece, R. J.; Maxwell A. *J. Biol. Chem.* **1989**, *264*, 19648-19653.
47. Larkin M. A.; Blackshields, G.; Brown, N. P.; Chenna, R.; McGettigan, P. A.; McWilliam, H.; Valentin, F.; Wallace, I. M.; Wilm, A.; Lopez, R.; Thompson, J. D.; Gibson, T. J.; Higgins, D. G. *Bioinformatics* **2007**, *23*, 2947-2948.
48. Cornell, W. D.; Cieplak, P.; Bayly, C. I.; Gould, I. R.; Merz, K. M. Jr.; Ferguson, D. M.; Spellmeyer, D. C.; Fox, T.; Caldwell, J. W.; Kollman, P. A. *J. Am. Chem. Soc.* **1995**, *117*, 5179-5197.
49. MOE (The Molecular Operating Environment) Version 2009.10, software available from Chemical Computing Group Inc., 1010 Sherbrooke Street West, Suite 910, Montreal, Canada H3A 2R7. <http://www.chemcomp.com>.
50. Olitzki, A. L.; Godinger, D.; Israeli, M.; Honigman A. *Appl Microbiol.* **1967**, *15*, 994-1001.